Based on the above analysis, the following pruning procedures are proposed.

(i) Train the network with the local EKF equations in an ascending order of $i$ and then a descending order of $n$.

(ii) Evaluate the sensitivity of each weight using eqn. 12 for all $i$, $k$ and $n$ and rank the importance of all the estimated weights according to their $\Delta E_k^n$. The ranking list is denoted by $\{S_1, S_2, ..., S_{N_w}\}$, with $\Delta E_{S_i} \leq \Delta E_{S_j}$ if $i < j$.

(iii) Set $\Delta \hat{w}_{S_k} = \hat{w}_{S_k}$ for $k = 1$ to $k'$ and $\Delta \hat{w}_{S_k} = 0$ for $k > k'$, and reform $\Delta \hat{w}_i^n$ by $\Delta \hat{w}_{S_k}$.

(iv) Estimate the incremental change in the mean prediction error due to the removal of the weights from $w_{S_1}$ up to $w_{S_k}$:

$$\Delta \mathbf{E}_{[S_1, S_{k'}]} = \sum_{n=1}^{M-1} \sum_{i=1}^{N_n} \delta(\Delta \hat{\mathbf{w}}_i^n)^T \mathbf{P}_i^n(\infty)^{-2} (\Delta \hat{\mathbf{w}}_i^n) \quad (13)$$

(v) If $\Delta \mathbf{E} \leq$ threshold, set $k' = k' + 1$ and go to step (iii). Otherwise, stop and remove the weights from $w_{S_1}$ up to $w_{S_{k'-1}}$ from the trained network.

*Simulation:* The proposed algorithm is applied to recognise handwritten digits. The sparse trace network of [3] with $20 \times 20$ input units, $14 \times 14$ hidden neurons and 10 output neurons is adopted here. The trace of the $i$th hidden unit for the $m$th class input patterns is defined as $T_{mi}(t) = \eta T_{mi}(t-1) + (1-\eta) x_i^h(t)$ [4], where $\eta$ is a control parameter, and $x_i^h(t)$ is the output of the $i$th hidden neuron. The hidden layer self-organises to extract the invariance of the input patterns according to the trace learning rule and eqns. 3 – 5 (in which the desired output $\mathbf{d}(t)$ is replaced with the trace $\mathbf{T}(t-1)$). The classifier, which consists of hidden and output layers, is trained by a local supervised EKF algorithm and categorises the input patterns using the extracted invariance. $5 \times 5$ input units are locally connected to the $i$th hidden neuron while the connection from the hidden to the output layer is global. The handwritten digit database previously used by Wallis [4] was adopted here. There are 20 sets of data (10 for training, the remaining 10 for testing) and each set contains 10 digits (from 0 to 9). We take $\mathbf{P}(0) = \mathbf{I}$ ($\mathbf{I}$ is the identity matrix) and $\eta = 0.7$. The initial traces $T(0)$ are fixed at zero.

Figs. 1*a* and *b* show the estimated and actual values of average square error against the number of weights pruned in the hidden and the output layer, respectively. The stopping criterion for the pruning process is set at a 2% increase in error. From the Figures, we observe that the estimated errors give an accurate prediction of the actual errors. Recognition rates for the training and the testing sets after 4040 weights (3460 in the hidden layer and 580 in the output layer) are removed are 100 and 70%, respectively, which are much higher than the results by Wallis (95 and 55%) as well as those by Peng (95 and 64.83%). The pruning processing improves the generalisation ability of the network.

*Conclusion:* The computational complexities per iteration are $O(5.0 \times 10^5)$ and $O(7.8 \times 10^7)$ for the local EKF training and pruning approaches, respectively. The corresponding storage requirements for training and pruning are both $O(5.0 \times 10^5)$. The computational costs for global EKF training and pruning are $O(4.7 \times 10^7)$ and $O(3.2 \times 10^{11})$, respectively, while the corresponding storage requirement is $O(4.7 \times 10^7)$ for both training and pruning. The local EKF algorithm requires a much lower computational complexity and storage requirement than the global one, which makes the local EKF training and pruning approach more practical for large-scale problems.


*18 October 2000*
*Electronics Letters Online No: 20010074*
*DOI: 10.1049/el:20010074*

Sheng-jiang Chang (*Institute of Modern Optics, Nankai University, Tianjin 300071, People's Republic of China*)

John Sum, Kwok-wo Wong and Chi-sing Leung (*Department of Electronic Engineering, City University of Hong Kong, Hong Kong*)

## References

1 IIGUNL, Y., SAKAI, H., and TOKUMARU, H.: 'Real-time learning algorithm for a multilayered neural network based on the extended Kalman filter', *IEEE Trans. Signal Process.*, 1992, **40**, pp. 959–967

2 SUM, J., LEUNG, C.S., YOUNG, G.H., and KAN, W.K.: 'On the Kalman filtering method in neural-network training and pruning', *IEEE Trans. Neural Netw.*, 1999, **10**, pp. 161–166

3 PENG, H., SHA, L., GAN, Q., and WEI, Y.: 'Energy function for learning invariant in multilayer perceptron', *Electron. Lett.*, 1998, **34**, pp. 292–294

4 WALLIS, G.: 'Using spatio-temporal correlations to learn invariant object recognition', *Neural Netw.*, 1996, **9**, pp. 1513–1519

# Demonstration of thermal poling in holey fibres

D. Faccio, A. Busacca, W. Belardi, V. Pruneri, P.G. Kazansky, T.M. Monro, D.J. Richardson, B. Grappe, M. Cooper and C.N. Pannell

A second-order nonlinearity is induced for the first time in a holey fibre by thermal poling. Non-phase matched second harmonic generation with a ~$10^{-8}$/W conversion efficiency is observed and the electro-optic coefficient is measured to be ~0.02pm/V.

*Introduction:* Thermal poling, first demonstrated in bulk silica-glass [1], is a well established technique for creating a second-order optical nonlinearity ($\chi^{(2)}$) in centro-symmetric materials. Soon after the first demonstration in bulk glass, a $\chi^{(2)}$ in thermally poled germano-silicate fibre was reported [2]. Despite the relatively low $\chi^{(2)}$ of 1pm/V, poled fibres represent an extremely attractive nonlinear medium, offering major advantages over more established crystalline materials in terms of waveguide length, damage threshold, loss and fabrication cost. On the other hand, holey fibres (HF), also known as photonic crystal or microstructured fibres, are of great interest for their unique waveguiding properties [3 – 5], many of which are important for nonlinear applications.

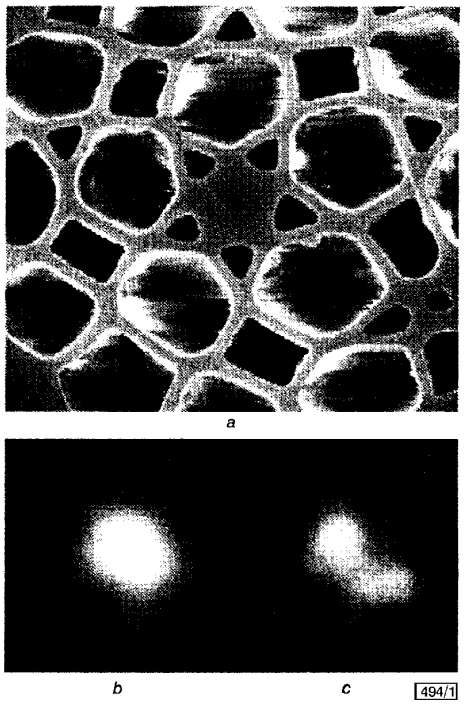


**Fig. 1** *Core region and mode profiles of thermally poled holey fibre*
*a* Core region of thermally poled holey fibre
*b* Mode profile of fundamental at 1550nm
*c* Mode profile of generated SHG at 775nm

Indeed, many applications based on these properties have already been studied for third-order nonlinear effects [6] and these may be extended to $\chi^{(2)}$ based phenomena. For example some HF designs

allow endlessly singlemode propagation [3] and our calculations also show that the overlap between interacting modes at widely different wavelengths can be further optimised so as to improve second-harmonic generation (SHG) efficiencies relative to conventional poled fibres. Moreover, we have found that the conversion bandwidth in a quasi-phase matched fibre may be significantly increased as a result of the greater flexibility for broadband waveguide-dispersion control [4]. Second-harmonic generation (SHG) due to surface effects has been observed in HFs [5], although we expect the nonlinearity induced by thermal poling to be much higher. However, the mechanism underlying thermal poling in silica glass is one of ionic migration which may not be possible in such a complex air:glass structure (see Fig. 1). In this Letter we demonstrate for the first time that thermal poling in HFs is indeed possible.

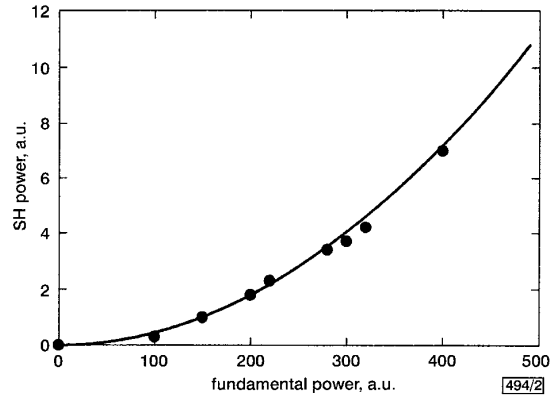


**Fig. 2** *Dependence of second harmonic (SH) on fundamental power*

● experimental data
——— best quadratic fit

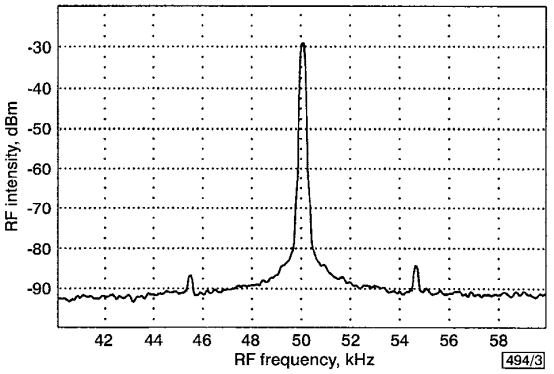


**Fig. 3** *RF spectrum from heterodyne Mach-Zehnder interferometer*

Holey fibre sample poled at 280°, 4kV for 30 minutes. Electro-optically induced phase shift was ~π/20 and electro-optic coefficient was 0.017pm/V

*Measurements and results:* The holey fibre had a guiding region as shown in Fig. 1*a*. The central core (6μm diameter) is made from Herasil-grade silica (from Heraeus) and is multimode at 1550nm, although in our experiments we were able to efficiently couple light into the fibre in such a way that at least 80% of the total power at 1550nm was in the fundamental mode, shown in Fig. 1*b*. The outer cladding structure (not shown in the Figure) has two holes 70μm apart into which the electrode wires were inserted. The nearest hole to the core was used to house the anode and is placed 27μm away from the guiding region. Note that if such a large anode-core separation were to be used in a standard fibre then the induced nonlinearity would not overlap with the core. A number of samples of the fibre were poled over a length of 7cm in air at 280°C for 30min and no dielectric breakdown was observed. The samples were then tested for SHG using 5W peak-power pulses of 200ns duration (1mW average power) from a 1550nm CW diode laser which was acousto-optically modulated at 1kHz and amplified in an Er-doped fibre amplifier. The coupling efficiency into the fibre was ~40%. SHG was absent in the untreated samples but was observed in all samples after poling although the signal varied greatly from one sample to the other due to the fact that the interaction was not phase-matched. We found a 1:4 ratio in the SH power generated between orthogonal pump polarisation states instead of the theoretical 1:9 ratio for a $C_{\infty v}$-symmetric nonlinearity induced by poling but this discrepancy may be well accounted for by the complex geometry of the HF. Fig. 2 shows the quadratic dependence of the SH on the fundamental power and the average conversion efficiency was estimated to be $10^{-8}$/W. Fig. 1*c* shows the SH mode profile, which is more similar to the $LP_{11}$ mode rather than to the $LP_{01}$ mode of the fundamental wavelength. To assess the actual value of the nonlinearity we carried out electro-optic measurements using a heterodyne Mach-Zehnder interferometer. The reference arm of the interferometer is modulated at 50kHz (carrier frequency) whereas the sample arm is modulated with a peak-to-peak voltage of ~150V at 3-5kHz, far from any mechanical resonances. The output from the interferometer is measured by a photodiode connected to an RF spectrometer — in the RF spectrum two sidelobes appear on either side of the carrier frequency, as shown in Fig. 3. The electro-optically induced phase shift in our samples was ~π/20 and we measured an electro-optic coefficient of 0.017pm/V, which, in silica, corresponds to $\chi^{(2)}$ ~0.04pm/V. This value, of the same order as that found in many germano-silicate fibres at 1.5μm, may be greatly increased by optimising the poling conditions and most of all the fibre geometry.

*Conclusions:* We have thermally poled for the first time a holey fibre and we have induced a second-order optical nonlinearity of the same order to that observed in many standard germano-silicate fibres. There is much room for improvement of this result. In particular, the distance between the anode electrode and the core region was not optimised in our fibre and careful design of the fibre geoemetry should lead to a significant increase in the nonlinearity reaching the same values observed in bulk silica, i.e. 1pm/V.

*Acknowledgments:* This research was supported by Pirelli Cables and Systems.


*23 November 2000*
*Electronics Letters Online No: 20010089*
*DOI: 10.1049/el:20010089*

D. Faccio, A. Busacca, V. Pruneri, P.G. Kazansky, T.M. Monro, W. Belardi and D.J. Richardson (*Optoelectronics Research Centre, Southampton University, Southampton, SO17 1BJ, United Kingdom*)

E-mail: dfaf@katamail.com

B. Grappe, M. Cooper and C.N. Pannell (*School of Physical Sciences, Kent University at Canterbury, Canterbury, CT2 7NR, United Kingdom*)

## References

1 MYERS, R.A., MUKHERJEE, N., and BRUECK, S.R.J.: 'Large second-order nonlinearity in poled fused silica', *Opt. Lett.*, 1991, **16**, (22), pp. 1732–1734

2 KAZANSKY, P.G., DONG, L., and RUSSELL, P.ST.J.: 'High second-order nonlinearities in poled silicate fibres', *Opt. Lett.*, 1994, **19**, (10), pp. 701–703

3 BIRKS, T.A., KNIGHT, J.C., and RUSSELL, P.ST.J.: 'Endlessly single-mode photonic crystal fiber', *Opt. Lett.*, 1997, **22**, (13), pp. 961–963

4 MONRO, T.M., RICHARDSON, D.J., BRODERICK, N.G.R., and BENNETT, P.J.: 'Holey optical fibres: an efficient modal model', *J. Lightwave Technol.*, 1999, **16**, pp. 923–928

5 RANKA, J.K., WINDELER, R.S., and STENTZ, A.J.: 'Optical properties of high-delta air-silica microstructure optical fibres', *Opt. Lett.*, 2000, **25**, (11), pp. 796–798

6 BRODERICK, N.G.R., MONRO, T.M., BENNETT, P.J., and RICHARDSON, D.J.: 'Nonlinearity in holey optical fibres: measurement and future opportunities', *Opt. Lett.*, 1999, **24**, (20), pp. 1395–1397